

See discussions, stats, and author profiles for this publication at: <https://www.researchgate.net/publication/279713066>

Energy-balance climate models

Chapter · January 2006

DOI: 10.1017/CBO9780511535857.004

CITATIONS
10

READS
1,873

2 authors:



Gerald R. North
Texas A&M University
234 PUBLICATIONS 11,011 CITATIONS

[SEE PROFILE](#)



Mark J Stevens
University of Colorado
56 PUBLICATIONS 1,099 CITATIONS

[SEE PROFILE](#)

Some of the authors of this publication are also working on these related projects:

-  Sustainability of Engineered Rivers in the Arid Lands [View project](#)
-  climate detection [View project](#)

3

Energy-balance climate models

GERALD R. NORTH AND MARK J. STEVENS

Department of Atmospheric Sciences, Texas A&M University, TAMU College Station, TX

3.1 Introduction

As discussed in Chapter 1, energy-balance climate models are important tools for studying Earth's climate. Energy-balance climate models (EBCMs) have been used in studies of climate change for more than a quarter of a century. Some papers can be found even before that, but the widespread use of these simple models was made popular by the nearly simultaneous appearance of the papers by Budyko (1968) and Sellers (1969). A review of these and other early works was presented in North *et al.* (1981). The purpose of this chapter is to introduce these models in the modern context, justifying their usefulness in certain situations without hiding their limitations. We also introduce stochastic versions of the models and some recent applications of them.

The EBCMs attempt to model Earth's surface-temperature field $T(\mathbf{r}, t)$, where \mathbf{r} is a point on the spherical surface and t is the time, by the constraint of energy conservation for individual columns of the Earth-atmosphere system. For each infinitesimal horizontal area element consider an ideal geometric column containing matter extending from roughly the tropopause to just beneath the solid Earth's surface, or to the bottom of the oceanic mixed layer, depending on location. The collection of all such columns covering Earth make up the system. It is assumed that the energetic indices of a column can be unambiguously labeled by the temperature at the surface (the column changes its temperature 'rigidly' from top to bottom). This is the first of a series of idealizations made in formulating the model. There are many fluxes of heat into and out of an individual column (now a box). Each of these fluxes is to be parameterized in terms of the surface temperature and its horizontal derivatives. Once the various fluxes into and out of a column are added

up and equated to the time rate of change of the energy content (sum of enthalpies of slabs in the vertical column) of the column (actually, all columns simultaneously), an equation emerges for the surface-temperature field as a function of position and time. This partial differential equation together with appropriate boundary conditions yields the surface-temperature field as a solution.

The steps in formulating the terms and the resulting equation will be presented briefly in the next section, but first one might ask why set up such a crude model of climate in the face of the progress being made in the construction of coupled ocean-atmosphere general-circulation models of today. First of all, in spite of the almost schematic formulation of the EBCMs they actually do a rather good job of representing the temperature field through the seasonal cycle and even in the fields of natural fluctuations, indicating that the larger scales of the surface-temperature field are insensitive to some of the dynamical details. Second, the models are amenable to a hierarchical formulation from global-average annual-average models to annual-average zonal-average models to two-dimensional seasonal models. This ability of running up and down the hierarchy provides an insight which proves useful. Finally, the models are subject to a certain amount of analytical treatment, allowing the old-fashioned methods of theoretical and statistical physics to be used in understanding the behavior of solutions. Solutions of EBCMs and their properties then form an intuitive framework or a benchmark with which to judge the outcomes of experiments with modern coupled ocean-atmosphere models of the climate system.

3.2 Formulation of EBCMs

In each of the following subsections a component of the energy budget is formulated.

3.2.1 Longwave radiation

Longwave radiation is the radiation energy per unit area per unit time leaving the top of the atmosphere going into space. It is concentrated in the infrared (IR) but the spectrum is complicated by several trace-gas absorbers/emitters in the atmosphere. Also at any one time about half the planet is covered with cloud, and the cloud tops emit roughly as black bodies which are at lower temperatures than the surface. Since the 1970s satellite sensors have been used to estimate the outgoing longwave radiation (Graves *et al.*, 1993). Budyko (1968) introduced a convenient parameterization, Equation (3.1), for the outgoing long wave flux, where T is in

$$F_{\text{LW}}(r, t) = A + BT(r, t) \quad (3.1)$$

$^{\circ}\text{C}$, A and B are empirical coefficients which can be fitted from satellite data of the outgoing flux $F_{\text{LW}}(\mathbf{r}, t)$ with the local surface temperature. The range of $T(\mathbf{r}, t)$ is provided by its climatology of latitude and seasonal dependence (month averages). The value of B is typically found to be $c.$ $1.90 \text{ W m}^{-2} \text{ }^{\circ}\text{C}^{-1}$; A is $c.$ 211 W m^{-2} (Graves *et al.*, 1993). The value of B is reasonably well defined in the middle latitudes but is essentially undetermined at low latitudes because of the poor dynamic range of T in the tropics and the fact that clouds are a significant determinant of F_{LW} at this latitude. Locally near the ITCZ there could even be an inverse relationship, since when local surface areas warm, clouds will form leading to less longwave radiation being lost to space from the cloud tops. Nevertheless, we will stick to our simple linear form, keeping in mind this potentially serious limitation.

There can also be a loss of energy flux by exchange with matter below the column usually in consideration. For example, over oceanic areas there is an exchange of heat with the deeper ocean below. This is typically taken to be linear with the difference between the mixed-layer temperature and the temperature of the layer just below it. In simulations one would find this indistinguishable from the simple $BT(r, t)$ term, but with B modified. It may thus be appropriate to use a larger value of B over oceanic areas to account for this phenomenon.

3.2.2 Shortwave radiation

Earth is heated by sunlight which is concentrated mainly in the visible part of the spectrum. The solar constant is the amount of radiation energy per unit time crossing a plane perpendicular to its path at the (annual average) Earth–Sun average distance; it is estimated to be about 1366 W m^{-2} . The amount of this energy impinging at the top of the atmosphere and averaged through the diurnal cycle is $QS(\mu, t)$, where Q is one quarter of the solar constant (because of the ratio of a sphere's area to that of a disk) and $S(\mu, t)$, where μ is the sine of latitude, is derived from elementary celestial mechanics. This function represents the fraction of the sunlight entering the atmosphere perpendicular to a surface element at a particular time of year (for a derivation see North *et al.*, 1981). By definition,

$$\int_0^1 S(\mu, t) d\mu = 1 \quad (3.2)$$

The planetary coalbedo is the fraction of the incoming solar beam that is absorbed by the system. In our case we are speaking of the coalbedo associated with the entire geometric column as opposed to say the surface coalbedo. The annual average

planetary coalbedo is defined by Equation (3.3), where t is in years, and ϕ is

$$a_p = \frac{1}{4\pi} \int_{-1}^1 \int_0^{2\pi} \int_0^1 a(\mu, \phi, t) S(\mu, t) dt d\phi d\mu \quad (3.3)$$

longitude. For Earth, the planetary coalbedo, a_p , is about 0.70.

The amount of radiation absorbed from sunlight per unit time can now be written as in Equation (3.4). Note that $a(\mathbf{r}, t)$ can have a dependence on position and time

$$F_{SW}(\mathbf{r}, t) = Q S(\mu, t) a(\mathbf{r}, t) \quad (3.4)$$

through the seasonal cycle or on other time scales. In particular there is a strong zenith-angle dependence especially over oceans. In fact, the coalbedo also depends upon such features as snowcover, clouds, etc, which can conceivably be parameterized by dependences on the surface-temperature field.

If we average over the planet and through the year, then equate the two fluxes, Equation (3.5), where T_{eq} is the mean annual planetary average temperature, which

$$A + B T_{eq} = Q a_p \quad (3.5)$$

can now be solved as in Equation (3.6). Using the values suggested earlier, we find

$$T_{eq} = \frac{Q a_p - A}{B} \quad (3.6)$$

$T_{eq} \approx 14.8^\circ\text{C}$, which is reasonably close to the observed value ($\approx 15^\circ\text{C}$). It might not be inappropriate to adjust the effective value of A downwards to force the global average temperature to agree with the observed value. This kind of fudging might be essential if one is hooking an icecap edge to a particular mean annual isotherm (e.g., Budyko's choice of -10°C).

3.2.3 Sensitivity

We can now calculate the rate of change of the planetary temperature with respect to a fractional change in solar constant, which we can think of as a control parameter, assuming a_p does not depend on T_{eq} , Equation (3.7). We find that this *static*

$$Q \frac{dT_{eq}}{dQ} = Q \frac{a_p}{B} = \frac{A + B T_{eq}}{B} \quad (3.7)$$

sensitivity is inversely proportional to B , the infrared damping coefficient. We say static sensitivity because in doing the change we wait for equilibrium to re-establish itself after the change in solar constant. The value of B seems to reflect the water-vapor feedback in the atmospheric column, but clouds are also involved. Using the

empirical values of A , B , a_p , Q , we find a static sensitivity of 1.26°C for a 1% increase in solar constant.

If Earth had no atmosphere and its surface behaved as a black body in the infrared, the value of B would exceed $4.61 \text{ W m}^{-2} \text{ }^\circ\text{C}^{-1}$. The smaller value of B for the real atmosphere appears to double the sensitivity. One must keep in mind however that the tropics (half Earth's surface) may well be misrepresented by our simple IR formula and it is likely that planetary sensitivity is reduced by tropical effects. Furthermore, in this simple estimate, we used the empirical value of a_p which includes the effect of cloud cover.

If the coalbedo depends on the temperature, we find the relationship shown in Equation (3.8). Hence, dependences of a_p on temperature through cloud, water

$$Q \frac{dT_{\text{eq}}}{dQ} = \frac{Q a_p}{B - Q \frac{da_p}{dT}} \quad (3.8)$$

vapor, or snow/ice cover can significantly increase or decrease sensitivity.

A crude way to take into account greenhouse-gas changes is through the parameter A . The dependence on CO_2 concentration is roughly given by Equation (3.9),

$$A(\text{CO}_2) = A_0 - 5.35 \ln \frac{C}{C_0} \quad (3.9)$$

where C is the CO_2 concentration in ppmv and C_0 is the present concentration (≈ 365 ppmv), and the coefficient $5.35 (\text{W m}^{-2})$ is derived from detailed radiative-transfer calculations (Myhre *et al.*, 1998). We can calculate the sensitivity to doubling CO_2 by calculating ΔT for $C = 2 \times C_0$, Equation (3.10).

$$\Delta T_{2 \times \text{CO}_2} = \frac{5.35 \ln(2)}{B} \approx 1.95^\circ\text{C} \quad (3.10)$$

Again, the important factor B appears in the denominator. And in the event that the coalbedo depends on T_{eq} we make the replacement $B \rightarrow B - \frac{da_p}{dT}$.

3.3 Time dependence

Before taking spatial dependences into account it is interesting to contemplate how the global average temperature responds to imbalances in the heat budget. For our schematic column of matter there is an effective heat capacity $C(r)$. The local magnitude of $C(r)$ will have a rather marked dependence on whether the local surface type is land or sea. For the moment consider an ideal geographically uniform planet in which case $C(r)$ is a constant independent of position. For the planet as a whole we can write Equation (3.11), where the subscript p denotes global average.

$$C \frac{dT_p}{dt} = Q a_p - A - B T_p \quad (3.11)$$

The solution of this simple initial value problem is given by Equation (3.12), where

$$T_p(t) = T_{\text{eq}} + (T_p(0) - T_{\text{eq}}) e^{-t/\tau} \quad (3.12)$$

the decay time constant is $\tau = C/B$. Again the replacement $B \rightarrow B - \frac{d\alpha_p}{dT}$ holds if albedo is allowed to depend on T ; however, if these dependences are included one must be mindful of the time constants of glacial growth, etc., which might enter, requiring separate governing equations which have to be coupled to the energy-balance equation through the temperature. The important point is that the relaxation time is proportional to the sensitivity ($\tau \propto \frac{1}{B}$): more sensitive climates will have longer relaxation times.

If the system is driven by a sinusoidal forcing of angular frequency ω , the response (take the real part at the end) is given by Equation (3.13); $T'(t)$ is the

$$\frac{dT'}{dt} + \frac{T'}{\tau} = \frac{F_\omega}{C} e^{-i\omega t} \quad (3.13)$$

departure from the time-independent steady-state solution. The steady-state response is similarly sinusoidal with complex amplitude, Equation (3.14), and the

$$|T_{p\omega}| = \frac{|F_\omega|}{B\sqrt{1+\omega^2\tau^2}} \quad (3.14)$$

phase lag (response lagging forcing) $\varphi = \arctan \omega\tau$. Note that even for infinite C the phase lag only reaches $\frac{\pi}{2}$ (quarter cycle). The response amplitude is inversely proportional to the damping coefficient B (larger sensitivity \rightarrow larger amplitude if τ is independently known). The amplitude decreases with frequency. Similarly the amplitude of the response is diminished and the phase lag is increased toward its upper limit of $\frac{\pi}{2}$ if τ is larger for a given value of B (maritime effect).

3.3.1 Random forcing

Weather instabilities and other small-scale effects cause temporal disturbances in the local heat balance, especially in mid latitudes. These disturbances cause the temperature field to fluctuate leading to the EBCM's version of natural variability. We introduce these disturbances through a stationary random function of time, $F(t)$. The autocovariance of this function diminishes very rapidly with time lag, being essentially a Dirac delta function, δ ; Equation (3.15). This kind of random

$$\langle F(t)F(t') \rangle = \sigma_F^2 \delta(t - t') \quad (3.15)$$

function in time is called *white noise*. The Fourier representation of such a function can be written as in Equation (3.16). The complex Fourier components F_ω are

$$F(t) = \frac{1}{2\pi} \int_{-\infty}^{\infty} F_{\omega} e^{-i\omega t} d\omega \quad (3.16)$$

random variables, with mean zero, statistically independent of one another at different ω and mean square $\langle |F_{\omega}|^2 \rangle$, a constant independent of ω . This means the power spectrum of the random forcing ($\propto \langle |F_{\omega}|^2 \rangle$) is *flat*.

We solved the response problem for a sinusoidal forcing at frequency ω in the last subsection. We can think of the white noise forcing as providing a sinusoidal term on the right-hand side of the energy-balance equation with a random amplitude at each frequency ω ; furthermore, the forcings at different frequencies are uncorrelated, a property of stationary time series. The solution for the amplitude of the temperature fluctuation is given by Equation (3.14) with T_{ω} now a normally distributed random variable. One finds that the power spectrum of the temperature (response) field is given by Equation (3.17). This is the typical *red noise* spectrum which for large ω

$$S_{\omega} = \langle |T_{\omega}|^2 \rangle = \frac{\langle |F_{\omega}|^2 \rangle}{B^2(1 + \omega^2\tau^2)} \quad (3.17)$$

goes as ω^{-2} .

Without going into details here one can also find the autocorrelation function, Equation (3.18), for the temperature field.

$$\rho(|t - t'|) = \exp\left(-\frac{|t - t'|}{\tau}\right) \quad (3.18)$$

In other words, the autocorrelation time (memory) for this process is precisely the relaxation time for the unforced EBCM. The value of τ for an all-land planet is just a month or so, while for a mixed-layer ocean planet (insulated from the deep ocean below) it is of the order of a few years. Note that this dependence of the autocorrelation function on τ permits its possible estimation independent of the knowledge of B and C separately through the study of the time series.

It is interesting to speculate that one might make an estimate of sensitivity, since if τ is known from time-series analysis, one might estimate the response amplitude to some known periodic forcing using Equation (3.14), then infer the sensitivity $\propto \frac{1}{B}$. A good candidate for the external periodic forcing is the approximately 11-year solar cycle (Stevens and North, 1996; North and Stevens, 1998).

3.3.2 Albedo feedback

The icecap feedback mechanism leads to some curious features of global climate. As a simple example, consider the case where the planetary coalbedo increases with global average temperature until all the ice disappears. Similarly as the temperature decreases the coalbedo decreases as the global average temperature decreases until

the icecap edge reaches the equator. Such a coalbedo function can lead to more than one solution of Equation (3.19). Typically, there is a solution similar to the

$$A + BT_{\text{eq}} = Qa_p(T_{\text{eq}}) \quad (3.19)$$

present climate with another solution at the same value of Q for which the planet is completely iced over. For reasonable dependences of a_p on T_{eq} a decrease of Q of c. 10% can lead to a catastrophic plunge to the ice-covered planet (North *et al.*, 1981; North, 1990; Mengel *et al.*, 1988; Lin and North, 1990). This appears to happen in GCMs as well as EBCMs.

3.4 Adding horizontal dimensions

If we consider an infinitesimal area element on the sphere and its heat budget, we must now take into account the divergence of heat flux leaving the area element due to advection. Also the heat capacity $C(\mathbf{r})$ as well as other macroscopic coefficients might depend on location or phase in the seasonal cycle. The simplest parameterization of heat flux is to take it proportional to the local temperature gradient: $-D(r)\nabla T(\mathbf{r}, t)$. The energy balance equation now becomes the partial differential Equation (3.20): Aside from the new term due to advection, there is a term F_{below}

$$C(\mathbf{r})\frac{\partial T}{\partial t} - \nabla \cdot (D(\mathbf{r})\nabla T) + A + BT = QS(x, t)a(\mathbf{r}, t; T) + F_{\text{below}} + F_{\text{noise}} \quad (3.20)$$

which is used to take into account fluxes into the oceanic mixed layer from below. This term essentially accounts for the poleward flow of heat in the oceans. It could be of the form $B'(r)(T - T_{\text{below}}(\mathbf{r}))$ or independent of temperature.

Use of diffusive heat transport always sparks debate. Two assertions of plausibility perhaps help. (1) At the coarsest scales most prevailing winds flow roughly along surface isotherms (i.e., $\mathbf{v} \cdot \nabla T \approx 0$). (2) The differences in time scale between atmospheric eddies (≈ 3 d) and the relaxation time of the surface-temperature field (≈ 1 month) is sufficient for the diffusion or random-walk approximation to hold at least in ensemble average. Some authors have suggested that the diffusion coefficient D should depend on temperature or its gradient, but this introduces a nonlinearity, which though small poses a complication best left out in our philosophical framework. In tuning to the present climate we do allow D to have a dependence on position, diminishing towards the poles.

3.4.1 Length scale

Just as $C/B = \tau$ is a representative time scale for global quantities, it is convenient to explore for a characteristic length scale at low frequency. This static length

scale turns out to be $\ell = \sqrt{D/B}$, which can be found in a variety of ways: decay of correlation in space for a randomly forced model, or the decay length of the response to a steady point heat source (Green's function). An interpretation of this length scale is the distance a randomly diffusing thermal anomaly goes during one characteristic decay time. The size of this scale is typically 1000 to 2000 km (for a comparison with data see Hansen and Lebedeff, 1987). It is, of course, dependent on the diffusive mechanism, but it means that features smaller than this length scale will be smeared out quickly. This length scale is curiously close to the Rossby radius in middle latitudes, but their relationship remains obscure.

If we cover Earth with disks of this radius we have only about 64 ($=8^2$) such 'statistically independent' areas. This means the standard deviation of a local temperature is about eight times that of the global average ($\approx 0.15^\circ\text{C}$ for annual averages). A gauge located at the center of each of these areas should give a good estimate of the global average temperature; i.e., the standard error of this estimate will be much less than the standard deviation of the planetary temperature. The standard error of a global average estimate based on well distributed point gauges will fall as the square root of the number of gauges, N , until we reach ~ 64 after which the reduction will be at a rate slower than $\propto 1/\sqrt{N}$. The latter occurs because when multiple gauges are located within one correlation radius of one another there is a degree of redundancy in the records.

The diffusive length scale may also play a role in the minimum size of stable icecaps. Dynamic features such as icecaps whose size is determined solely by the temperature field smaller than this length tend to be unstable. Hence, ice sheets tend to be larger than this size or not at all. This has led to conjecture that icecaps such as those on Greenland, Antarctica, or the Laurentide ice sheets might have formed rather suddenly. Actually, only the conditions for growth are sudden – it takes thousands of years to build the ice thickness. On the other hand, ice sheets can disappear rather quickly once the critical size for instability is reached (Lindzen and Farrell, 1977; North, 1984).

3.4.2 Seasonal cycle

Next we wish to show that the seasonal cycle of the surface-temperature field can be represented rather well with such a simple model. In doing so there are two approaches. The first is to demonstrate that the essential physics is captured by the energy balance (for an example, see North *et al.*, 1983). In this approach we keep the number of free parameters in the problem at a minimum. A second approach is to drop the parsimonious parameter issue and tune the phenomenological coefficients in the EBCM to all available data in order to use the model in applications – this is discussed in a later section. Returning to the first approach, for example, we

drop the term F_{below} and let $D(\mathbf{r})$ take on a very simple form dependent only on latitude, mildly decreasing toward the poles and symmetric across the equator. The heat capacity takes on one value over land and another over ocean (two orders of magnitude larger), the latter suppressing the seasonal amplitude and increasing the phase lag over the oceans. Moreover, we drop the temperature dependence of the coalbedo, making the problem entirely linear (but to see interesting effects of allowing the snowline to enter, see North *et al.*, 1983; Mengel *et al.*, 1988; Lin and North, 1990; Hyde *et al.*, 1990). In this case the seasonal cycle is composed of a seasonal mean, an annual harmonic, and a semiannual harmonic. This is a very rapidly converging Fourier series, with the semiannual harmonic being everywhere less than c. 2 °C, while the annual harmonic peaks at near 30 °C over the interior of the large continents. Similarly the phase lag of the seasonal cycle is only about a month over the continents and near a quarter cycle over the oceans. These fields have been shown to be in qualitatively good agreement with the corresponding ones from the data by North *et al.* (1983) and Hyde *et al.* (1990).

A similar agreement is found for the fields of variance and covariance (from one site to another) of climate fluctuations for month averages as well as for longer time averages (Kim and North, 1991; 1992). In the parsimonious parameter approach we take the noise forcing to be uniform over the globe and white in both space and time. In this way, only one free parameter is introduced in the noise – its overall variance or strength. Because of the land–sea heat capacity variation over the planet, we find large variance over the continents and small variance over the oceans, with a smooth transition joining them which has a length scale of ℓ . The comparisons with data and some general circulation model (GCM) output can be found in a series of papers by Kim, North and colleagues (Kim and North, 1991; 1992; Leung and North, 1991; North *et al.*, 1992). In the comparisons of EBCM solutions for the steady-state seasonal cycle and for the second moment fluctuation statistics it can be seen that there is reasonable basis to believe that the EBCM is capturing the main physics at these space and time scales for the surface-temperature field.

3.4.3 Comparison with GCM simulations

In a series of papers using an early version of the NCAR Community Climate Model an attempt was made to check the EBCM in some controlled situations. To facilitate the comparisons the boundary conditions in the GCM were simplified to a planet called “Terra Blanda.” Terra Blanda consists of a planet with no geographical/seasonal features: no topography, all-land, equinox or mean annual forcing, north–south symmetric, no ice-albedo effect, no soil-moisture memory. This set of conditions allowed considerable savings in the computer time necessary to

gather essential statistics. For instance, one could treat all longitudes as statistically equivalent as well as all months. By having no ocean, the longest radiation relaxation time is about one month. The EBCM for this configuration is solvable analytically with spherical harmonics (North and Cahalan, 1981; Leung and North, 1991). A control run with the GCM showed that the sequence of relaxation times for the different spatial scales (spherical harmonic degrees) of the GCM solution matched those of the EBCM quite well (Leung and North, 1991). Similarly the spatial-length scales were in good agreement between the models.

In a comprehensive study comparing the two model solutions, it was shown that the power spectrum of the Terra Blanda simulations with the GCM were very similar to those of the EBCM. Finally, the response of the GCM to point and latitudinal-ring heat sources was also in close agreement (North *et al.*, 1992).

3.4.4 Tuned simulations with EBCMs

A reasonable analogy to the above approach to EBCMs is the Bohr model of the atom or the shell model in nuclear physics. We know the model is somewhat schematic and based upon some questionable assumptions. On the other hand, there is clearly a physical basis for the validity of the model. In addition the EBCMs form an extremely useful intuitive introduction and guide to the problem, especially considering the incredible complexity of the real climate system and the GCMs being developed for simulations. The fact that there are only a few free or adjustable parameters in EBCMs makes it hard to cheat by fudging more coefficients than there are actual data to be fitted. This will always be a problem for the large complex models since there is never enough data to constrain all the phenomenological coefficients in the sub-grid scale parameterizations. Scientific testing of models becomes problematic since new data sets that might be used for model testing are very rapidly incorporated in the tuning of the next generation of the model.

The above discussion suggests that EBCMs can be used as a tool in certain applications where only the surface temperature is needed. Also the EBCMs are so cheap to run over long periods they can be used as a laboratory to test such notions as sampling errors when only short segments or a few realizations from GCM simulations are available. It therefore behoves us to relax the criterion of as few adjustable parameters as possible, so that we can achieve the best possible fit to observations in order to use the EBCM in these applications. For this reason in the following tuning exercise we allow some additional dependences in the parameterizations. These are physically motivated, but hardly derived rigorously from a set of fundamental principles. The most direct example is to allow the diffusion coefficient to have different values over land and ocean, to allow the

noise forcing to be peaked in the middle latitudes, etc. We also allow the heat from below the mixed layer to have a latitude dependence until the mean annual surface-temperature field is in good agreement with observations. This flux from below is fixed and does not affect climate-change calculations or fluctuation statistics.

Figures 3.1 and 3.2 show some results obtained when the EBCM is tuned to reproduce the current climatology as well as possible given the model's limitations. Figure 3.1a shows the amplitude of the annual harmonic of the surface-temperature field for the tuned model, while Figure 3.1b shows that derived from the observed climatology. The lag of the surface temperature after the solar forcing at the top of the atmosphere (TOA) is shown for both the model (Figure 3.2a) and the observed climatology (Figure 3.2b). Some spatial properties of the statistics of the noise-forced EBCM temperature field are shown in Figures 3.3–3.5. Figure 3.3 shows the one-year lag autocorrelation of the annual mean surface temperature for the model (Figure 3.3a) and observed data (Figure 3.3b). The variance field for the annual mean surface temperature is shown in Figure 3.4. Finally, Figure 3.5 shows the square of the correlation of the local annual mean surface temperature with grid points selected from Asia (Figures 3.5a,b), and the North Atlantic (Figures 3.5c,d). While these figures reveal some of the shortcomings of the EBCM, they also show how well such a simple model can simulate the basic statistical properties of the surface temperature.

3.5 Applications

A rather fruitful area for making use of the EBCM is in the estimation of parameters in the climate system. Since the EBCM can be solved quickly by standard numerical methods, the statistics of the solution fields can be easily obtained. Furthermore, one can establish the sampling errors incurred if only short records or only a few realizations are available.

3.5.1 Paleoclimatology

The ability to modify quickly and run EBCMs to an equilibrium solution make them natural choices for paleoclimate studies. Much of the earlier research using EBCMs was concerned with the investigation of the causes of the ice ages (North *et al.*, 1983; Short *et al.*, 1991; Crowley *et al.*, 1992). This is still a topic of more recent research (Crowley and Kim, 1994), as well as the investigation of climate forcings over the past few hundred years (Crowley and Kim, 1996; 1999). The EBCMs have also been useful for modeling the more distant past (North and Crowley, 1985; Crowley *et al.*, 1986; Crowley and Kim, 1995).

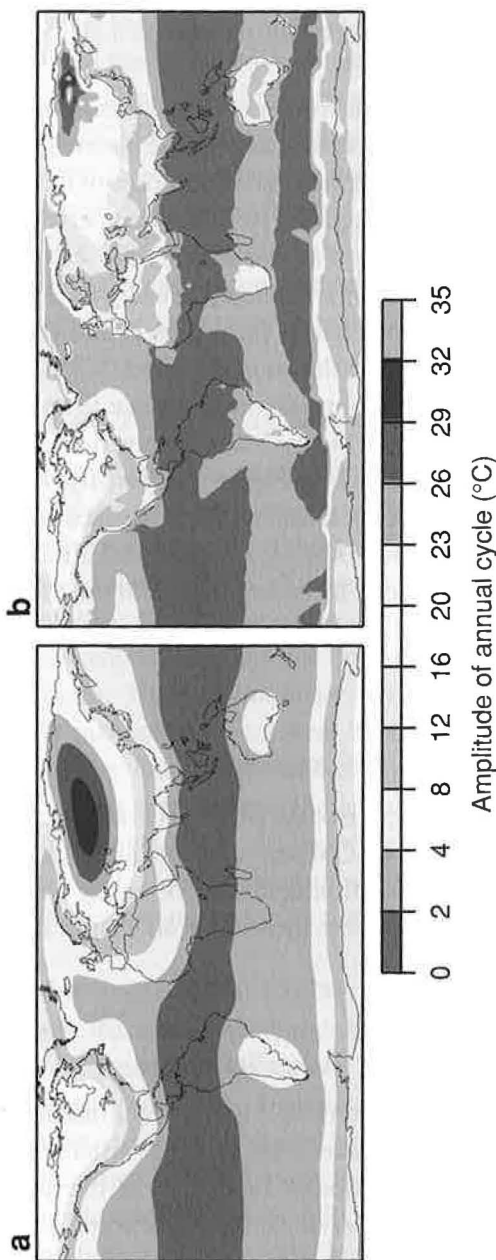


Figure 3.1. Amplitude of annual cycle of surface temperature computed using 40 years of EBCM control-run data (a), and observed climatology (b).

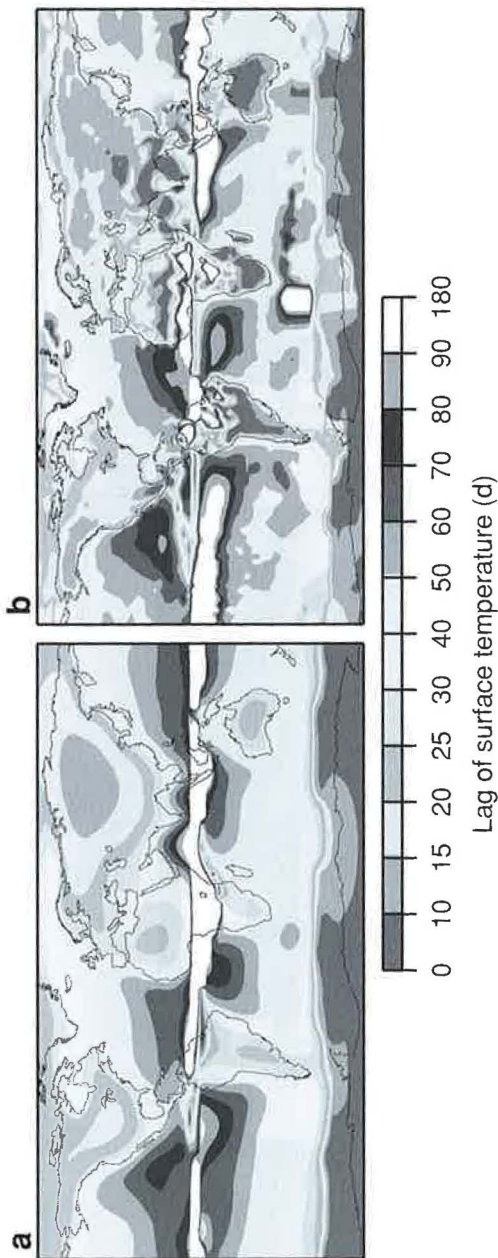


Figure 3.2. Lag of surface temperature after TOA solar forcing computed using 40 years of EBCM control-run data (a), and observed climatology (b).

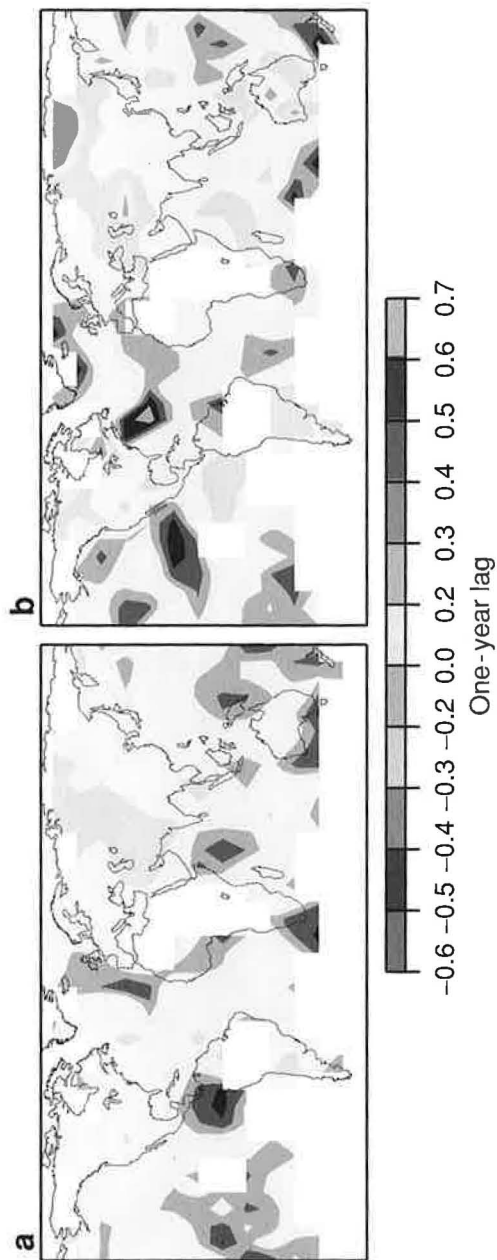


Figure 3.3. One-year lag autocorrelation of annual mean surface temperature computed using 40 years of EBCM control-run data (a), and 40 years of detrended observations 1958-97 (b).

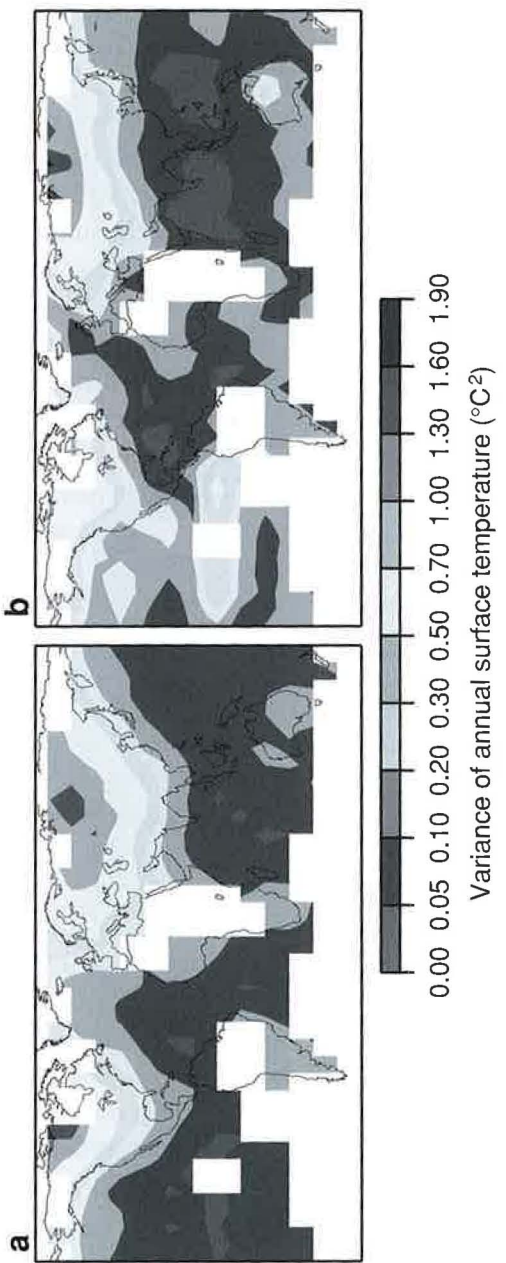


Figure 3.4. Variance of annual mean surface temperature computed using 40 years of EBCM control-run data (a), and 40 years of detrended observations 1958–97 (b).

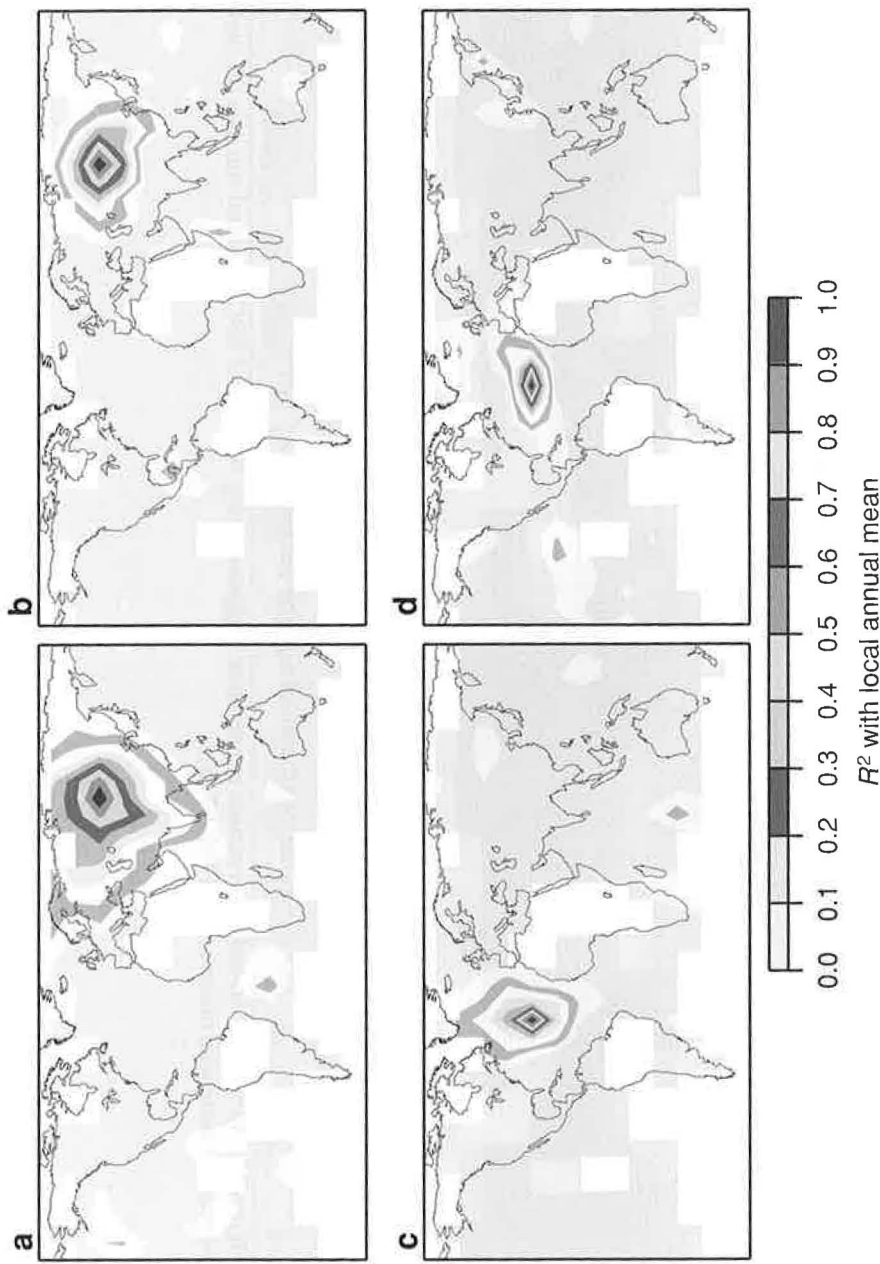


Figure 3.5. Square of the correlation of the local annual mean surface temperature with a grid point in Asia (50° N, 90° E) using 40 years of EBCM control data (a), and detrended observations 1958–97 (b), similarly for a point in the North Atlantic (30° N, 40° W) using EBCM data (c), and observations (d).

3.5.2 Estimation of area averages and other aggregates

A problem of great interest is the errors incurred in estimating a global or hemispheric average from data based on a finite number of point measurements. The errors will depend upon the variance field, the space-time autocorrelation structure and the averaging time. Energy-balance climate models have been used to study this problem and have shown that surprisingly few stations are required to obtain a rather good estimate of the global average temperature (Shen *et al.*, 1994). By good we mean that the sampling error (standard error) is actually much smaller than the natural variability. If the station data are optimally weighted as few as 16 stations are capable of obtaining a satisfactory estimate of the global average. Similar studies have been conducted to find the standard error in estimating spherical harmonic coefficients (Zwiers and Shen, 1997). One can also estimate the spherical harmonic power spectrum (variance of the spherical harmonic coefficients). Because the number of point sites is finite, there will be aliasing biases in the estimates (Li *et al.*, 1997). Li and North (1998) have studied the problem of sampling error and bias when estimating area averages and spherical harmonic amplitudes from polar orbiting satellites.

3.5.3 Signal detection in the climate system

Energy-balance climate models have been used in the study of signal detection in the current climate-change debate (North *et al.*, 1995; North and Kim, 1995; Stevens and North, 1996; North and Stevens, 1998). In this problem one hypothesizes that there are four forced signals in the 100-year record of surface temperatures: greenhouse gases (G), anthropogenic aerosols (A), solar cycle forcing (S), and volcanic aerosols (V). Simulations of the 100 years for each of these forcings is conducted and the EBCM responses form the signals. One then proceeds to use these space-time signal patterns as the regression variables in a multiple regression exercise. The question is, in fitting the observations to these signals, what are the amplitudes of the individual signals, and what are their statistical error properties. For instance, one wishes to know if the null hypothesis that the amplitude G is zero can be rejected at a certain confidence level. One might also ask what the actual amplitude of A is including its confidence interval.

Several GCM groups are working on this problem and one might ask why bother with such a crude tool as the EBCM? The answer is simple, one cannot obtain a 'clean' signal from a GCM, since it is inevitably contaminated with sampling error itself. One must run many realizations of the 100-year forced GCM run for each signal. With the EBCM this is trivial, since one merely turns off the noise forcing to obtain a signal pattern. In fact, one can study the error (bias) incurred

from using only a few realizations of the signal runs. In the regression problem it is customary to use long control runs to establish the covariance statistics of the temperature field. Typically these control runs are of 1000-year duration. With the EBCM one can easily make control runs of 10 000 years to establish the sampling error incurred in the shorter control runs. Several studies have now been conducted with the EBCM signals along with a comparative study of natural variability of several GCM control runs. The results for amplitude estimation do not seem to depend very sensitively on the choice of model used in the control runs (North and Stevens, 1998).

3.6 Conclusion

Energy-balance climate models provide a simple introduction to the main physical principles of global climate. The largescale fields including the seasonal cycle and natural fluctuation statistics are rather well simulated by these simple models. Not only are the models easy to understand and provide insight into the various processes involved, they have proven useful in some applications especially those involving statistical sampling error and signal processing studies.

Of course, these models have a number of limitations which must be acknowledged. The models are thermal balance models: they do not provide winds and they seem to only work well near the surface where largescale wave phenomena are strongly damped. They cannot include ocean dynamics beyond the simple upwelling diffusion models (Kim *et al.*, 1992). The EBCM considers the vertical profile of the atmosphere to be rigid not allowing changes in lapse rate or other potential feedbacks which might be important. Clouds are treated only through the macroscopic coefficients A , B , and a . For the most part cloud feedback is ignored. Water-vapor feedback is included empirically in the damping coefficient B , but this is probably only valid for mid latitudes.

References

- Budyko, M. I. (1968). The effect of solar radiation variations on the climate of the Earth. *Tellus* **21**, 611–19.
- Crowley, T. J. and K.-Y. Kim (1994). Milankovitch forcing of the last interglacial sea level. *Science* **265**, 1566–8.
- (1995). Comparison of longterm greenhouse projections with the geologic record. *Geophys. Res. Lett.* **22**, 933–6.
- (1996). Comparison of proxy records of climate change and solar forcing. *Geophys. Res. Lett.* **23**, 359–62.
- (1999). Modeling the temperature response to forced climate change over the last six centuries. *Geophys. Res. Lett.* **26**, 1901–4.

- Crowley, T. J., K.-Y. Kim, J. G. Mengel, and D. A. Short (1992). Modeling 100,000-year climate fluctuations in pre-Pleistocene time series. *Science* **255**, 705–7.
- Crowley, T. J., D. A. Short, J. G. Mengel, and G. R. North (1986). Role of seasonality in the evolution of climate during the last 100 million years. *Science* **231**, 579–84.
- Graves, C. E., W.-H. Lee, and G. R. North (1993). New parameterizations and sensitivities for simple climate models. *J. Geophys. Res.* **98**, 5025–36.
- Hansen, J. and S. Lebedeff (1987). Global trends of measured surface air temperature. *J. Geophys. Res.* **92**, 13345–72.
- Hyde, W. T., K.-Y. Kim, T. J. Crowley, and G. R. North (1990). On the relation between polar continentality and climate: Studies with a nonlinear seasonal energy balance model. *J. Geophys. Res.* **95**, 18653–68.
- Kim, K.-Y. and G. R. North (1991). Surface temperature fluctuations in a stochastic climate model. *J. Geophys. Res.* **96**, 18573–80.
- (1992). Seasonal cycle and second-moment statistics of a simple coupled climate system. *J. Geophys. Res.* **97**, 20437–48.
- Kim, K.-Y., G. R. North, and J. Huang (1992). On the transient response of a simple coupled climate system. *J. Geophys. Res.* **97**, 10069–81.
- Leung, L.-Y. and G. R. North (1990). Information theory and climate prediction. *J. Clim.* **3**, 5–14.
- (1991). Atmospheric variability on a zonally symmetric land planet. *J. Clim.* **4**, 753–65.
- Li, T.-H. and G. R. North (1998). Sampling errors for meteorological fields observed by low Earth orbiting satellites. *J. Geophys. Res.* **103**, 19595–614.
- Li, T.-H., G. R. North, and S. S. Shen (1997). Aliased power of a stochastic temperature field on a sphere. *J. Geophys. Res.* **102**, 4475–86.
- Lin, R. Q. and G. R. North (1990). A study of abrupt climate change in a simple nonlinear climate model. *Clim. Dyn.* **4**, 253–61.
- Lindzen, R. S. and B. Farrell (1977). Some realistic modifications of simple climate models. *J. Atmos. Sci.* **34**, 1487–1501.
- Mengel, J. G., D. A. Short, and G. R. North (1988). Seasonal snowline instability in an energy balance model. *Clim. Dyn.* **2**, 127–31.
- Myhre, G., E. J. Highwood, K. P. Shine, and F. Stordal (1998). New estimates of radiative forcing due to well mixed greenhouse gases. *Geophys. Res. Lett.* **25**, 2715–18.
- North, G. R. (1984). The small ice cap instability in diffusive climate models. *J. Atmos. Sci.* **41**, 3390–5.
- (1990). Multiple solutions in energy balance climate models. *Paleogeog., Paleoclim., Paleoecol.* **82**, 225–35.
- North, G. R. and R. F. Cahalan (1981). Predictability in a solvable stochastic climate model. *J. Atmos. Sci.* **38**, 504–13.
- North, G. R. and T. J. Crowley (1985). Application of a seasonal climate model to Cenozoic glaciation. *J. Geol. Soc. London* **142**, 475–82.
- North, G. R. and K.-Y. Kim (1995). Detection of forced climate signals. Part II: simulation results. *J. Clim.* **8**, 409–17.
- North, G. R. and M. J. Stevens (1998). Detecting climate signals in the surface temperature record. *J. Clim.* **11**, 563–77.
- North, G. R., R. F. Cahalan, and J. A. Coakley (1981). Energy balance climate models. *Rev. Geophys. Space Phys.* **19**, 91–121.
- North, G. R., J. G. Mengel, and D. A. Short (1983). Simple energy balance model resolving the seasons and the continents: application to the astronomical theory of the ice ages. *J. Geophys. Res.* **88**, 6576–86.

- North, G. R., K.-Y. Kim, S. S. Shen, and J. W. Hardin (1995). Detection of forced climate signals. Part I: filter theory. *J. Clim.* **8**, 401–8.
- North, G. R., K.-J. Yip, L.-Y. Leung, and R. M. Chervin (1992). Forced and free variations of the surface temperature field in a general circulation model. *J. Clim.* **5**, 227–39.
- Sellers, W. D. (1969). A global climatic model based on the energy balance of the Earth-atmosphere system. *J. Appl. Meteor.* **8**, 392–400.
- Shen, S. S. P., G. R. North, and K.-Y. Kim (1994). Spectral approach to optimal estimation of the global average temperature. *J. Clim.* **7**, 1999–2007.
- Short, D. A., J. G. Mengel, T. J. Crowley, W. T. Hyde, and G. R. North (1991). Filtering of Milankovitch cycles by Earth's geography. *Quat. Res.* **35**, 157–73.
- Stevens, M. J. and G. R. North (1996). Detection of the climate response to the solar cycle. *J. Atmos. Sci.* **53**, 2594–608.
- Zwiers, F. W. and S. S. Shen (1997). Errors in estimating spherical harmonic coefficients from partially sampled GCM output. *Clim. Dyn.* **13**, 703–16.